IEEE Transactions on Pattern Analysis and Machine Intelligence

Disclaimer: "Relative Fuzzy Connectedness and Object Definition: Theory, Algorithms, and Applications in Image Segmentation"

A claim of priority in research and publication appeared on page 1486 in the paper "Relative Fuzzy Connectedness and Object Definition: Theory, Algorithms, and Applications in Image Segmentation" by J.K. Udupa, P.K. Saha and R.A. Lotufo (*IEEE Transactions on Pattern Analysis and Machine Intelligence*, vol. 24, no. 11, pp. 1485-1500, Nov. 2002) with respect to the paper "Multiseeded Segmentation Using Fuzzy Connectedness" by G.T. Herman and B.M. Carvalho (*IEEE Transactions on Pattern Analysis and Machine Intelligence*, vol. 23, no. 5, pp. 460-474, May 2001). Furthermore, the wording of this claim suggests professional misconduct on the part of G.T. Herman and B.M. Carvalho.

Responsibility for the content of published papers rests with the authors. The peer review process is intended to determine the overall significance of the technical contribution of a manuscript. The peer review process does not provide a way to validate every statement in a manuscript. In particular, the IEEE has not validated the claim referred to in the first paragraph above. The IEEE regrets publishing this unauthenticated statement and the pain that such publication may have caused to G.T. Herman and B.M. Carvalho.

Relative Fuzzy Connectedness and Object Definition: Theory, Algorithms, and Applications in Image Segmentation

Jayaram K. Udupa, *Senior Member*, *IEEE*, Punam K. Saha, *Member*, *IEEE*, and Roberto A. Lotufo

Abstract—The notion of fuzzy connectedness captures the idea of "hanging-togetherness" of image elements in an object by assigning a strength of connectedness to every possible path between every possible pair of image elements. This concept leads to powerful image segmentation algorithms based on dynamic programming whose effectiveness has been demonstrated on 1,000s of images in a variety of applications. In the previous framework, a fuzzy connected object is defined with a threshold on the strength of connectedness. In this paper, we introduce the notion of relative connectedness that overcomes the need for a threshold and that leads to more effective segmentations. The central idea is that an object gets defined in an image because of the presence of other co-objects. Each object is initialized by a seed element. An image element c is considered to belong to that object with respect to whose reference image element c has the highest strength of connectedness. In this fashion, objects compete among each other utilizing fuzzy connectedness to grab membership of image elements. We present a theoretical and algorithmic framework for defining objects via relative connectedness and demonstrate utilizing the theory that the objects defined are independent of reference elements chosen as long as they are not in the fuzzy boundary between objects. An iterative strategy is also introduced wherein the strongest relative connected core parts are first defined and iteratively relaxed to conservatively capture the more fuzzy parts subsequently. Examples from medical imaging are presented to illustrate visually the effectiveness of relative fuzzy connectedness. A quantitative mathematical phantom study involving 160 images is conducted to demonstrate objectively the effectiveness of relative fuzzy connectedness.

Index Terms—Fuzzy connectedness, image segmentation, object definition, digital topology.

1 Introduction

Two and higher-dimensional images are currently available through sensing devices that operate on a wide range of frequency in the electromagnetic spectrum—from ultrasound to visible light to X and γ-rays [1]. Defining objects in these image data is fundamental to most computerized image-related applications. It is obvious that defining objects is essential prior to their visualization, manipulation, and analysis. Even operations such as image interpolation and filtering, seemingly unrelated to object definition, can be made more effective with object knowledge. Thus, defining objects in images seems to be vital to any computerized operation that is done on images.

This activity, generally referred to as image segmentation, spans over three decades [2]. There are many general theories and solutions proposed to deal with this problem. While these are valuable in seeking insight into this difficult problem, making them work in a given application with a proven level of precision, accuracy, and efficiency usually requires a considerable amount of work. On the other hand, theories and solutions motivated entirely by specific applications have also been developed. The present paper falls in this latter category and deals with an extension of a previous work [3] which was also motivated by the problem of defining objects in multidimensional medical images.

Object definition in images may be considered to consist of mainly two related tasks—recognition and delineation. *Recognition* is the process of determining roughly the whereabouts of the object in the image. *Delineation*, on the other hand, is a process that defines the precise spatial extent and composition of the object in the image. The points in an object exhibit usually a gradation of image intensities. This is usually due to artifacts, blurring, and background variations introduced by the imaging devices as well as due to heterogeneity of the actual object material property itself. Complete automation of segmentation in the sense of performing recognition and delineation automatically has remained a challenge in many application areas, especially in biomedical imaging. As a consequence, a variety of approaches have been taken wherein the degree of automation for recognition and delineation falls in between completely manual to completely automatic.

Among automatic approaches to recognition, two classes may be identified: knowledge-based and model-based. Knowledge-based methods (for example, [4], [5]) form hypotheses relating to objects and test them for recognizing object parts. Usually, some preliminary delineation is needed for forming and testing hypotheses relating to object components. Model-based methods (for example, [6],

- *J.K. Udupa and P.K. Saha are with the Medical Image Processing Group, Department of Radiology, University of Pennsylvania, Fourth Floor, Blockley Hall, 418 Service Dr., Philadelphia, PA 19104-6021. E-mail: {jay, saha}@mipg.upenn.edu.*
- *R.A. Lotufo is with the Department of Engineering, Compuacao e Automacao Industrial, Universidade Estadual de Campinas, Unicamp, Faculdade de Engenharia Eletrica, Caixa Postal 6101, Campinas-SP-13081-970, Brazil. E-mail: lotufo@dca.fee.unimp.br.*

Manuscript received 15 Nov. 2000; revised 17 Sept. 2001; accepted 14 Apr. 2002.
Recommended for acceptance by S. Sarkar.
For information on obtaining reprints of this article, please send e-mail to: tpami@computer.org, and reference IEEECS Log Number 113149.

[7], [8]) utilize predefined object models to optimally match image information to models for recognizing object components.

Approaches to delineation may be broadly classified into two groups: boundary-based and region-based. Boundary-based methods (for example, [9], [10], [11]) produce a delineation of the object boundaries in the image whereas region-based methods (for example, [12], [13], [14]) generate delineations in the form of the region occupied by the object in the image. Each of these groups may be further divided into subgroups—hard and fuzzy—depending on whether the defined regions/boundaries are described by hard or fuzzy sets.

The subject matter of this paper is related to delineation. In a previous paper [3], we described a theory and algorithms for fuzzy connected object definition, treating a given image as a fuzzy subset of the set of spatial image elements (spels) comprising the image. In short, the approach consists of defining a "local" fuzzy relation called *affinity* on the set of spels. The affinity value assigned to a pair of spels is based on how close the spels are spatially and in terms of intensity and intensity-based properties. A "global" fuzzy relation called *connectedness* is defined on the set of spels based on affinity. The connectedness value assigned to a pair (c, d) of spels is the strength of the strongest of all paths from c to d. The "strength" of a path is simply the smallest affinity along the path. It was shown that fuzzy connectedness is a similitude relation and that the fuzzy components defined by this relation are an appropriate choice for characterizing objects in images. It was also shown that, in spite of its enormous combinatorics, fuzzy component extraction can be done computationally elegantly via dynamic programming. This is an established method which is currently routinely utilized in several medical imaging applications including multiple sclerosis lesion segmentation and quantification [15], [16], [17], MR angiography [18], [19], mammographic density quantification [20], and, hard and soft tissue 3D imaging for craniofacial surgery [21]. Thousands of 3D images have been successfully processed in these applications. The motivations for the development of this method came from two considerations. First, spels in an object region usually have a gradation of intensity values in an image. Second, in spite of this graded composition of spel intensities, spels hang together (form gestalts) to define an object. The basis for [3] was our belief that both these aspects—graded composition and hanging togetherness of spels—should be handled in a fuzzy setting. Although the aspect of graded composition has been addressed abundantly in the image processing literature, the aspect of hanging-togetherness has been addressed mostly in the sense of hard connectedness relations among spels. Since hard connectedness requires a binary segmentation first, it does not allow the flexibility afforded by fuzzy connectedness to define object entities with a range of strength of hanging-togetherness. This fuzzy spatio-topological concept provides a vital piece of information regarding objects that is ignored by published fuzzy segmentation strategies such as the clustering techniques [22], [23]. This fuzzy topological information leads to more effective segmentation under various conditions of material heterogeneity, background variations and noise. See [24], [25], [26] for earlier publications on fuzzy connectedness, [24] being the first to introduce this notion. Our treatment in [3] was fundamentally different from that in [24] in several essential ways including the translation of the theoretical results into practical segmentation algorithms.

In the present paper, an extension to the definition of fuzzy objects described in [3] is proposed. Instead of defining an object on its own based on the strength of connectedness, all co-objects of importance that are present in the image are also considered and the objects are let to compete among themselves in having spels as their members. In this competition, every pair of spels in the image will have a strength of connectedness in each object. The object in which this strength is highest will claim membership of the spels. This approach to fuzzy object definition using relative strength of connectedness eliminates the need for a threshold of strength of connectedness that was part of the previous definition. It seems to be more natural since it relies on the fact that an object gets defined in an image by the presence of other objects that coexist in the image. Its theory and an iterative extension are presented in Sections 2 and 3, respectively. In Section 4, we present the associated algorithms. In Section 5, some examples are presented, including an objective evaluation based on 160 phantom images, to illustrate the behavior of relative connectedness especially as compared to the previous definition [3] . Finally, concluding remarks are stated in Section 6. In this paper, we confine ourselves to the case of two objects to simplify the theory. A multi object generalization of this theory and algorithms has recently been developed [27]. The key ideas of this paper were previously presented at conferences [28], [29].

Some comments regarding the origin of the relative fuzzy connectedness ideas and their iterative version as described in Section 3 of this paper are in order. To the best of our knowledge, the first recorded disclosure of these ideas was the submission of an abstract by us to the SPIE International Symposium on Medical Imaging in August 1998. This subsequently appeared as a paper in the conference proceedings [28]. In the mean time, Udupa presented a seminar on 14 December 1998 at the Medical Image Processing Group, University of Pennsylvania, Philadelphia, in which he described the full results contained in the present paper. A related paper, [30] whose key idea is also relative fuzzy connectedness. The authors of paper [30] were present at the December 1998 seminar mentioned above and started working in 1999 in the same research group on the results presented in [30]. The latter was submitted to *IEEE Transactions on Pattern Analysis and Machine Intelligence* prior to the submission of the present manuscript to the same journal. In addition to the fact that the key idea of [30] is relative fuzzy connectedness (whose originators are clearly the authors of the present manuscript), the theoretical results of [30] are particular cases of the results described in the present paper. Additionally, our results establish the conditions under which the resulting segmentations are guaranteed to be independent of the seed points, and the algorithms guarantee the repeatability of

segmentation. The results of [30] cannot assure the repeatability of segmentations. Further, unlike [30], our algorithms have been evaluated on mathematical phantoms and have been tested and have already been utilized in several clinical applications on 100s of patient studies.

2 Theory of Relative Fuzzy Connectedness

The terminology of [3] is followed throughout in this paper. For completeness, some of the key concepts from [3] that are required in this paper are briefly described first. Prior to this, an intuitive description of the key ideas is given using a two-dimensional example.

2.1 An Outline of the Key Ideas

Consider a 2D image composed of two regions corresponding to two objects O_1 and O_2 as illustrated in Fig. 1, O_2 being the background. O_2 itself may consist of multiple objects among which we are not interested in distinguishing since our object of interest is O_1. In the rest of this paper, therefore, we consider everything other than the object of interest as the background. Suppose we determine an affinity relation that assigns to every pair of nearby spels in the image a value based on the nearness of spels in space and in intensity (or in features derived from intensities). Affinity represents local "hanging togetherness" of spels. To every "path" connecting every pair of spels, such as the solid curve p_{co_1} connecting c and o_1 in Fig. 1, a "strength of connectedness" is assigned which is simply the smallest pairwise affinity of spels along the path. The strength of connectedness between any two spels such as o_1 and c is simply the strength of the strongest of all paths between o_1 and c. Suppose p_{co_1} shown in Fig. 1 represents the strongest path between o_1 and c. If the affinity is designed properly, then p_{co_1} is likely to have a higher strength than the strength of any path such as the dotted curve between c and o_1 that goes outside O_1.

In the original fuzzy connected method [3], an object such as O_1 is segmented by setting a threshold on the strength of connectedness. This threshold defines a pool of spels such that within this pool the strength of connectedness between any two spels is not less than the threshold but between any two spels, one in the pool and the other not in it, the strength is less than the threshold. The basic idea in relative fuzzy connectedness is to first select reference spels o_1 and o_2, one in each object, and then to determine to which object any given spel belongs based on its relative strength of connectedness with the reference spels. A spel c, for example, would belong to O_1 since its strength of connectedness with respect to o_1 is likely to be greater than that with o_2. This relative strength of connectedness offers a natural mechanism for partitioning spels into regions based on how the spels hang together among themselves relative to others. A spel such as a in the boundary between O_1 and O_2 will be grabbed by that object with whom a hangs together most strongly. This mechanism not only eliminates the need for a threshold required in the original method but also offers potentially more powerful segmentation strategies for two reasons. First, it allows more direct utilization of the information about all objects in the image in determining the segmentation of a given object. Second, considering from a point of view of thresholding the strength of connectedness, it allows adaptively changing the threshold depending on the strength of connectedness of objects that surround the object of interest.

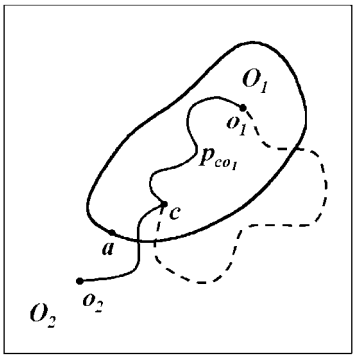

Fig. 1. Illustration of the main ideas behind relative fuzzy connectedness. The membership of any spel, such as c, in an object is determined based on the strength of connectedness of c with respect to the reference spels o_1 and o_2 specified in objects O_1 and O_2. c belongs to that object with respect to whose reference spel it has the highest strength of connectedness.

In Sections 2.2-2.5, we briefly reproduce from [3] some basic definitions and results that are needed for later developments in this paper.

2.2 Fuzzy Subsets, Fuzzy Relation [31]

Let X be any reference set. A *fuzzy subset* $\mathcal{A}$ of X is a set of ordered pairs $\mathcal{A} = \{(x, \mu_{\mathcal{A}}(x)) \mid x \in X\}$, where $\mu_{\mathcal{A}} : X \to [0,1]$ is the *membership function* of $\mathcal{A}$ in X. We say $\mathcal{A}$ is *nonempty* if there exists $x \in X$ such that $\mu_{\mathcal{A}}(x) \neq 0$. The empty fuzzy subset of X, denoted Φ, satisfies $\mu_{\Phi}(x) = 0$ for all $x \in X$. In this paper, Φ is used to denote the empty fuzzy subset of any reference set, ϕ is used to denote the empty hard set, and μ subscripted by a fuzzy subset is used to always denote the membership function. A *fuzzy relation* ρ *in* X is a fuzzy subset of $X \times X$

$$\rho = \{((x,y), \mu_\rho(x,y)) \mid x, y \in X\},$$

where $\mu_\rho : X \times X \to [0,1]$. Let ρ be any fuzzy relation in X. ρ is said to be *reflexive* if, $\forall x \in X,\ \mu_\rho(x,x) = 1$; *symmetric* if, $\forall x, y \in X,\ \mu_\rho(x,y) = \mu_\rho(y,x)$; *transitive* if,

$$\forall x, z \in X,\ \mu_\rho(x,z) = \max_{y \in X}[\min[\mu_\rho(x,y), \mu_\rho(y,z)]].$$

ρ is called a *similitude relation* in X if it is reflexive, symmetric, and transitive. The analogous concept for hard binary relations is an *equivalence relation*.

2.3 Fuzzy Spel Adjacency, Fuzzy Digital Space, Scene, Binary Scene, Segmentation

Let n-dimensional Euclidean space R^n be subdivided into hypercuboids by n mutually orthogonal families of parallel hyperplanes. Assume, with no loss of generality, that the hyperplanes in each family have equal unit spacing so that the hypercuboids are unit hypercubes, and we shall choose coordinates so that the center of each hypercube has integer coordinates. The hypercubes will be called *spels* (an abbreviation for "space elements"). When $n = 2$, spels are called *pixels*, and when $n = 3$ they are called *voxels*. The

coordinates of a center of a spel are an n-tuple of integers, defining a point in Z^n. Z^n itself will be thought of as the set of all spels in R^n with the above interpretation of spels, and the concepts of spels and points in Z^n will be used interchangeably.

A fuzzy relation α in Z^n is said to be a *fuzzy spel adjacency* if it is reflexive and symmetric. It is desirable that α be such that $\mu_\alpha(c,d)$ is a nonincreasing function of the distance $|c-d|$ between c and d, where $|\cdot|$ represents any $L2$ norm in R^n. The pair (Z^n,α), where α is a fuzzy spel adjacency, will be referred to as a *fuzzy digital space*. Fuzzy digital space is a concept that characterizes the underlying digital grid system independent of any image-related concepts.

A *scene over* a fuzzy digital space (Z^n,α) is a pair $\mathcal{C}=(C,f)$, where $C=\{c \mid -b_j \le c_j \le b_j \text{ for some } b \in Z_+^n\}$, Z_+^n is the set of n-tuples of positive integers, f, called *scene intensity*, is a function whose domain is C, called *scene domain*, and whose range is a set of numbers. Any scene $\mathcal{C}$ over (Z^n,α) in which the range of f is a subset of $[0,1]$ is called a *membership scene over* (Z^n,α). $\mathcal{C}$ is a *binary scene over* (Z^n,α) if $\mathcal{C}$ is a membership scene over Z^n in which the range of f is $\{0,1\}$.

n-segmentation is any process that converts a scene over (Z^n,α) to a binary scene over (Z^n,α). *n-fuzzy segmentation* is any process that converts a scene over (Z^n,α) to a membership scene over (Z^n,α). The purpose of n-segmentation may be considered as to delineate the object of interest as a hard subset of the scene domain. The purpose of n-fuzzy segmentation may be thought of as to delineate the object of interest as a fuzzy subset of the scene domain. In the binary case, the membership is all or none. In the fuzzy case, the membership scene intensity of the spels indicates the amount of object material present in the spel or the degree of belongingness of the spel in the object.

2.4 Fuzzy Spel Affinities, Path, Fuzzy κ-Net

Let $\mathcal{C}=(C,f)$ be a scene over (Z^n,α). Any fuzzy relation κ in C is said to be a *fuzzy spel affinity* (or, *affinity* for short) *in* $\mathcal{C}$ if it is reflexive and symmetric. The intent here is that κ should depend on, in addition to the spatial nearness of spels, their intensities and other features. In practice, κ should be such that, for any $c,d \in C$, $\mu_\kappa(c,d)$ is a function of:

1. the fuzzy adjacency of c and d,
2. the homogeneity of the spel intensities at c and d,
3. the closeness of the spel intensities and of the intensity-based features of c and d to some expected intensity and feature values for the object,
4. the actual location of c and d (i.e., μ_κ may be shift variant).

Some examples of μ_κ are given in [3], and a detailed comparative study of a variety of functional forms for μ_κ is reported in [32] including a scale-based formulation. A typical form of μ_κ that we have used in this paper and in our previous works is as follows:

$$\mu_\kappa(c,d)=\mu_\alpha(c,d)\sqrt{\mu_\psi(c,d)\mu_\phi(c,d)}, \tag{2.1}$$

where μ_α is the hard 4- (in 2D) or 6- (in 3D) adjacency relation, μ_ψ is the homogeneity component of affinity, and μ_ϕ is the object feature component. μ_ψ is such that $\mu_\psi(c,d)$ is greater when c and d belong locally to the same homogeneous region. It is enough to consider homogeneity alone in determining affinity (see [32]). Effective affinities require that the intensity features around c and d should also be considered. $\mu_\phi(c,d)$ is greater when these intensity features are closer to an expected value of the features for the object. A detailed description on how to devise μ_ψ and μ_ϕ has been reported in [32]. In evaluating both μ_ψ and μ_ϕ, all voxels in the vicinity of c and d determined by the scale at c and d are considered. The scale at any spel c is the radius of the largest hyperball centered at c within which the scene intensity is homogeneous. The idea of space-variant local scale used here [32] is different from the multiscale strategies commonly used. A few other studies on local scale have been reported from different research groups [33], [34], [35], [36]. It is clear that μ_κ should depend on all three factors—μ_α, μ_ψ, and μ_ϕ. Equation (2.1) is one of several forms that satisfy the requirements imposed on κ and that seem to give the best results based on our studies. A complete description of μ_ψ and μ_ϕ will take a considerable amount of space and, therefore, will not be provided here. We refer the reader to [32] for a thorough study of how to devise affinities. Throughout this paper, κ with appropriate subscripts and/or superscripts will be used to denote fuzzy spel affinities.

Let $\mathcal{C}=(C,f)$ be a scene over a fuzzy digital space (Z^n,α) and let κ be an affinity in $\mathcal{C}$. A *path* p_{cd} *in* $\mathcal{C}$ *from* a spel c *to* a spel d is any sequence $\langle c_1,c_2,\cdots,c_m\rangle$ of $m \ge 2$ spels in C such that $c_1=c$ and $c_m=d$. Note that the successive spels in the sequence may be any elements of C. The set of all paths in $\mathcal{C}$ from c to d is denoted by P_{cd}. The set of all paths in $\mathcal{C}$, defined as $\bigcup_{c,d\in C} P_{cd}$, is denoted by $P_{\mathcal{C}}$. The *fuzzy* κ*-net* $\mathcal{N}_\kappa$ *of* $\mathcal{C}$ is a fuzzy subset of $P_{\mathcal{C}}$ with its membership function defined as follows. For any path

$$p_{cd}=\langle c=c_1,c_2,\cdots,c_m=d\rangle \in P_{\mathcal{C}},$$

$$\mu_{\mathcal{N}_\kappa}(p_{cd})=\min_{1\le i<m}[\mu_\kappa(c_i,c_{i+1})]. \tag{2.2}$$

The fuzzy κ-net concept captures the idea of assigning a "strength" to every path that connects any pair of spels in $\mathcal{C}$. For any $S \subseteq C$, we say that the path p_{cd} is *contained in* S if all spels of p_{cd} belong to S.

2.5 Fuzzy κ-Connectedness, Fuzzy $\kappa\theta$-Object, κ-Connectivity Scene

Let $\mathcal{C}=(C,f)$ be a scene over (Z^n,α), let κ be an affinity in $\mathcal{C}$, and let $\mathcal{N}_\kappa$ be the fuzzy κ-net of $\mathcal{C}$. *Fuzzy* κ*-connectedness in* $\mathcal{C}$, denoted K, is a fuzzy relation in C, defined as follows. For all $c,d \in C$, $\mu_K(c,d)=\max_{p_{cd}\in P_{cd}}[\mu_{\mathcal{N}_\kappa}(p_{cd})]$. Throughout this paper, the upper case form of the symbol used to represent a fuzzy spel affinity will be used for the corresponding fuzzy connectedness.

The following proposition, proven in [3], is vital for the rest of the paper.

Proposition 2.1. *For any scene* $\mathcal{C}$ *over* (Z^n,α)*, for any affinity* κ *in* $\mathcal{C}$*, fuzzy connectedness* K *in* $\mathcal{C}$ *is a similitude relation in* C.

For any $\theta \in [0,1]$, consider a hard binary relation K_θ defined as follows. For any $c,d \in C$, $\mu_{K_\theta}(c,d)=1$, if $\mu_K(c,d) \ge \theta$, and 0 otherwise. It can be shown [3] that K_θ is an equivalence

relation. For any $o \in C$, let $[o]_{K_\theta}$ denote the equivalence class of K_θ in C that contains o. A *fuzzy $\kappa\theta$-object $\mathcal{O}$ of $\mathcal{C}$ containing o* is a fuzzy subset of C such that, for any $c \in C$, $\mu_{\mathcal{O}}(c) = \eta(f(c))$, if $c \in [o]_{K_\theta}$, and 0 otherwise. Here, η is a function that maps the imaged intensity values into objectness values. In n-segmentation (binary), we simply set $\eta(f(c)) = 1$. In n-fuzzy segmentation, η may be chosen to be a Gaussian whose mean and standard deviation correspond to the intensity value expected for the object region and its standard deviation (or some multiple there of). The choice of η should depend on the particular imaging modality that generated $\mathcal{C}$ and the object under consideration. The intuitive idea underlying the notion of a fuzzy $\kappa\theta$-object $\mathcal{O}$ is the following. Through K, we have defined a strength of connectedness (hanging-togetherness) between all possible pairs of spels in C in an object that contains o. For a specified threshold θ, the mask (support) O of $\mathcal{O}$ consists of a pool of spels such that, within this pool, the strength of connectedness between every two spels is at least the threshold value. For any spel outside the pool, its strength of connectedness with any spel inside the pool is less than the threshold. In other words, O represents a maximal pool of spels that contains o such that the spels in this pool hang together at a strength at or above the threshold.

If we proceed directly from the definition, computing fuzzy $\kappa\theta$-objects in $\mathcal{C}$ becomes computationally impractical even for 2D scenes. The following theorem, proven in [3], provides a practical solution for this task via dynamic programming, as demonstrated in [3].

Theorem 2.2. *For any scene $\mathcal{C} = (C, f)$ over (Z^n, α), for any affinity κ in $\mathcal{C}$, and for any spel $o \in C$, the fuzzy $\kappa\theta$-object $\mathcal{O}$ containing o is given by the following membership function. For any $c \in C$, $\mu_{\mathcal{O}}(c) = \eta(f(c))$, if $\mu_K(o, c) \geq \theta$, and $\mu_{\mathcal{O}}(c) = 0$ otherwise.*

The notion of a connectivity scene, that gives a map of the strength of connectedness of all spels of $\mathcal{C}$ with respect to a reference spel, is important for the rest of this paper. For any scene $\mathcal{C} = (C, f)$ over (Z^n, α), for any affinity κ in $\mathcal{C}$, and for any spel $o \in C$, the *κ-connectivity scene of o in $\mathcal{C}$* is the scene $\mathcal{C}_{K_o} = (C, f_{K_o})$ such that for any,

$$c \in C, f_{K_o}(c) = \mu_K(o, c).$$

Theorem 2.2 suggests that the fuzzy $\kappa\theta$-object of $\mathcal{C}$ containing o can be computed by determining the κ-connectivity scene of o in $\mathcal{C}$ and then by thresholding this scene at θ. Although our aim in this paper is not determining fuzzy $\kappa\theta$-objects, computing the κ-connectivity scene is essential for delineating objects via relative fuzzy connectedness.

2.6 Relative Fuzzy κ-Object

For any spels o, b in C, define

$$P_{ob_\kappa} = \{c \mid c \in C \text{ and } \mu_K(o, c) > \mu_K(b, c)\}. \quad (2.3)$$

The idea here is that o and b are typical spels specified in "object" and "background," respectively. Note that $P_{ob_\kappa} = \phi$, if $b = o$.

A *fuzzy κ-object $\mathcal{O}$ of a scene $\mathcal{C} = (C, f)$ containing a spel o relative to a background containing a spel b* is the fuzzy subset of C defined by the following membership function. For any $c \in C$,

$$\mu_{\mathcal{O}}(c) = \begin{cases} \eta(f(c)), & \text{if } c \in P_{ob_\kappa}, \\ 0, & \text{otherwise.} \end{cases} \quad (2.4)$$

For short, we will refer to $\mathcal{O}$ as simply a *relative fuzzy κ-object* of $\mathcal{C}$. The following proposition states a fundamental property of the relationship of the strength of fuzzy connectedness among any three spels.

Proposition 2.3. *For any scene $\mathcal{C} = (C, f)$ over (Z^n, α), for any affinity κ in $\mathcal{C}$, and for any spels c, d, e all in C, let $s_1 = \mu_K(c, d)$, $s_2 = \mu_K(d, e)$, and $s_3 = \mu_K(e, c)$. Then,*

$$\begin{aligned} &\text{for some } i \neq j \neq k, \text{ and } i, j, k \in \{1, 2, 3\}, \\ &\text{we have } s_i = s_j \leq s_k. \end{aligned} \quad (2.5)$$

Proof. Suppose $\mu_K(c, d) > \mu_K(d, e) = s$. Then, by the transitivity of K (Proposition 2.1),

$$\mu_K(e, c) \geq \min[\mu_K(c, d), \mu_K(d, e)] = s.$$

However, $\mu_K(e, c) \not> s$, because, otherwise, by transitivity of K, $\mu_K(d, e) = s \geq \min[\mu_K(c, d), \mu_K(e, c)] > s$, which contradicts our assumption. Thus, whenever

$$\mu_K(c, d) > \mu_K(d, e), \mu_K(e, c) = \mu_K(d, e).$$

On the other hand, if $\mu_K(c, d) = \mu_K(d, e)$ then,

$$\mu_K(e, c) \geq \mu_K(c, d) = \mu_K(d, e).$$

Since, c, d, e are any spels of C, the proof is complete. □

Some particular cases of a relative fuzzy κ-object are instructive to study. Suppose $\mu_K(b, o) = 1$. Then, by (2.3) and (2.5), $P_{ob_\kappa} = \phi$ and the relative κ-object is empty. This makes sense since both o and b are inside the "object" in this case and there is no meaningful separation between sets of spels "hanging together" with o and with b. Note also that, when $\mathcal{C}$ is a binary scene and $f(o) \neq f(b)$, i.e., $\mu_K(o, b) \neq 1$, then P_{ob_κ} is essentially a connected component of spels whose type is that of o that contains o (assuming that κ is appropriately chosen). To ensure that the definition in (2.3) and (2.5) is reasonable, we will establish several properties of relative fuzzy κ-object. The most important among these is that, for any spel q in P_{ob_κ} and most spels r not in P_{ob_κ}, we get the same relative fuzzy κ-object. This property becomes essential in routine applications wherein an operator has to specify the initial seed spels in the object and in the background. It is impractical for different human operators (or for the same operator at different times) to specify the "same" seed spels. However, it is easy for these different specifications to guarantee that the seed spels are in the same object and background regions. It will be unacceptable if these different seed specifications result in different n segmentations, implying nonrepeatability of the method. Our theory guarantees the repeatability. This property has neither been investigated nor satisfied by the method of [30]. We now proceed to establish this robustness result.

Proposition 2.4. *For any scene $\mathcal{C} = (C, f)$ over (Z^n, α), for any affinity κ in $\mathcal{C}$, and for any spels o, b, q and c in C such that $q \in P_{ob_\kappa}$,*

$$\mu_K(q, c) > \mu_K(b, c) \quad (2.6)$$

if, and only if, $c \in P_{ob_\kappa}$.

Proof. Suppose $\mu_K(q,c) \leq \mu_K(b,c)$. Then, by (2.5),

$$\mu_K(b,q) \geq \mu_K(q,c).$$

This implies $\mu_K(o,q) > \mu_K(q,c)$ since $q \in P_{ob_\kappa}$ and so $\mu_K(o,q) > \mu_K(b,q)$. By (2.5), therefore, $\mu_K(q,c) = \mu_K(o,c)$. This implies that $\mu_K(b,c) \geq \mu_K(o,c)$ which then implies that $c \notin P_{ob_\kappa}$.

To prove the converse, suppose $\mu_K(q,c) > \mu_K(b,c)$. Then, by (2.5), $\mu_K(b,q) = \mu_K(b,c)$. This implies

$$\mu_K(o,q) > \mu_K(b,c),$$

since $q \in P_{ob_\kappa}$ and so $\mu_K(o,q) > \mu_K(b,q)$. Following similitudity of fuzzy connectedness,

$$\mu_K(o,c) \geq \min[\mu_K(o,q), \mu_K(q,c)] > \mu_K(b,c).$$

Hence, $c \in P_{ob_\kappa}$. □

Note that the above result is not valid if "$\geq$ " is used in (2.3) instead of "$>$ ".

Proposition 2.5. *For any scene $\mathcal{C} = (C, f)$ over (Z^n, α), for any affinity κ in $\mathcal{C}$, and for any spels o, b, q, c and r in C such that $q, c \in P_{ob_\kappa}$ and $r \in \overline{P}_{ob_\kappa} = C - P_{ob_\kappa}$,*

$$\mu_K(b,o) = \mu_K(b,c) = \mu_K(b,q), \tag{2.7}$$
$$and, \mu_K(r,o) = \mu_K(r,c) = \mu_K(r,q). \tag{2.8}$$

Proof. Equation (2.7) follows directly from the fact that $q, c \in P_{ob_\kappa}$ and by (2.5) and (2.6).

To prove (2.8), note that since

$$r \in \overline{P}_{ob_\kappa}, \mu_K(r,o) \leq \mu_K(b,r).$$

By (2.5), this implies that

$$\mu_K(b,o) \geq \mu_K(r,o). \tag{2.9}$$

Since $\mu_K(o,c) > \mu_K(b,c)$, by (2.7),

$$\mu_K(o,c) > \mu_K(b,o). \tag{2.10}$$

By (2.9) and (2.10), $\mu_K(r,o) < \mu_K(o,c)$. Hence, by (2.5), $\mu_K(r,o) = \mu_K(r,c)$. Analogously, we can show that $\mu_K(r,o) = \mu_K(r,q)$. □

Proposition 2.6. *For any scene $\mathcal{C} = (C, f)$ over (Z^n, α), for any affinity κ in $\mathcal{C}$, and for any spels o, b, q, c, and, r in C such that $q, c \in P_{ob_\kappa}$ and $r \in \overline{P}_{ob_\kappa} = C - P_{ob_\kappa}$,*

$$\mu_K(q,c) > \mu_K(r,c). \tag{2.11}$$

Proof. Suppose $\mu_K(q,c) \leq \mu_K(r,c)$. This implies, by (2.5), that $\mu_K(r,q) \geq \mu_K(q,c)$. Combining with (2.8), we have

$$\mu_K(r,o) \geq \mu_K(q,c). \tag{2.12}$$

Since $r \notin P_{ob_\kappa}$, $\mu_K(r,o) \leq \mu_K(r,b)$, which, by (2.5), implies that

$$\mu_K(b,o) \geq \mu_K(r,o). \tag{2.13}$$

From (2.12) and (2.13), we have

$$\mu_K(b,o) \geq \mu_K(q,c). \tag{2.14}$$

Combining (2.14) and (2.6), $\mu_K(b,o) > \mu_K(b,c)$. Hence, from (2.5), $\mu_K(b,c) = \mu_K(o,c)$, which is a contradiction to our initial assumption that $c \in P_{ob_\kappa}$. □

Unfortunately, (2.11) is not a sufficient condition for the membership of c in P_{ob_κ} as we will show later.

Proposition 2.7. *For any scene $\mathcal{C} = (C, f)$ over (Z^n, α), for any affinity κ in $\mathcal{C}$, and for any spels o, b and q in C such that $q \in P_{ob_\kappa}$, $P_{qb_\kappa} = P_{ob_\kappa}$.*

Proof. Suppose $c \in P_{ob_\kappa}$. By (2.6), $\mu_K(q,c) > \mu_K(b,c)$. By (2.3), hence $c \in P_{qb_\kappa}$.

Suppose $c \in P_{qb_\kappa}$. Since $q \in P_{ob_\kappa}$, we have

$$\mu_K(o,q) > \mu_K(b,q).$$

By (2.7), $\mu_K(o,q) > \mu_K(o,b)$ so that $o \in P_{qb_\kappa}$. Hence, by (2.6),

$$\mu_K(o,c) > \mu_K(b,c)$$

and by (2.6), $c \in P_{ob_\kappa}$. □

This proposition asserts the robustness of the relative fuzzy κ-object to the reference spel selected in the object region. However, constancy of the κ-object with respect to reference spels specified in the background requires more constraints, as indicated by the following theorem.

Theorem 2.8. *For any scene $\mathcal{C} = (C, f)$ over (Z^n, α), for any affinity κ in $\mathcal{C}$, and for any spels o, b, q and r in C such that $q \in P_{ob_\kappa}$,*

$$P_{ob_\kappa} = P_{qr_\kappa}, if\ r \in P_{bo_\kappa}. \tag{2.15}$$

Proof. Let $r \in P_{bo_\kappa}$ and let $c \in P_{ob_\kappa}$. By (2.11), $\mu_K(q,c) > \mu_K(r,c)$ which implies $c \in P_{qr_\kappa}$.

Now, let $c \in P_{qr_\kappa}$. By (2.3), $\mu_K(q,c) > \mu_K(r,c)$. Since

$$r \in P_{bo_\kappa},\ \ \mu_K(o,r) < \mu_K(b,r),$$

which, by (2.5), implies $\mu_K(o,r) = \mu_K(b,o)$. We claim that $o \in P_{qr_\kappa}$. This is because $\mu_K(o,q) > \mu_K(b,q)$ since $q \in P_{ob_\kappa}$, and by (2.5), $\mu_K(o,q) > \mu_K(b,o)$ which implies

$$\mu_K(o,q) > \mu_K(r,o).$$

Hence, by (2.6), $\mu_K(o,c) > \mu_K(r,c)$, which implies (by (2.5))

$$\mu_K(o,c) > \mu_K(o,r) = \mu_K(b,o).$$

Therefore, by (2.5), $\mu_K(o,c) > \mu_K(b,c)$ and, hence, $c \in P_{ob_\kappa}$. □

Note that the condition in (2.15) is sufficient (for $P_{ob_\kappa} = P_{qr_\kappa}$) but not necessary. The necessary and sufficient condition is expressed in the following theorem.

Theorem 2.9. *For any scene $\mathcal{C} = (C, f)$ over (Z^n, α), for any affinity κ in $\mathcal{C}$, and for any spels o, b, q and r in C such that $q \in P_{ob_\kappa}$,*

$$P_{ob_\kappa} = P_{qr_\kappa}\ if,\ and\ only\ if, \mu_K(b,o) = \mu_K(r,o). \tag{2.16}$$

Proof. Suppose $\mu_K(b,o) = \mu_K(r,o)$. Then, by (2.5),

$$\mu_K(b,r) \geq \mu_K(o,r),$$

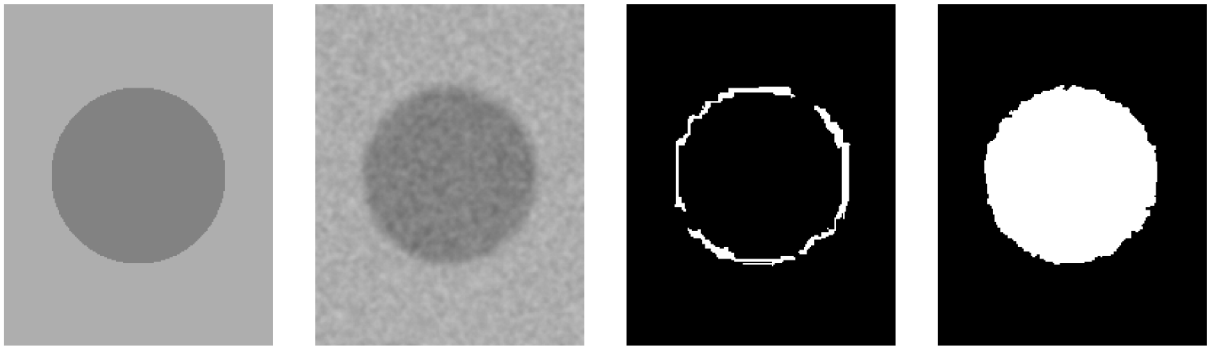

Fig. 2. (a) A binary scene of a disk. (b) The scene of (a) after introducing a blur (via Gaussian smoothing), noise and a background component of variation. (c) The set of spels (white) for which the conditions expressed in (2.15) and (2.16) are violated. (d) The set P_{ob_κ} (white) when o is chosen to be near the center of the circular disk, and b is chosen deep in the background.

which implies that $r \notin P_{ob_\kappa}$. Hence, by (2.11), $\mu_K(q,c) > \mu_K(r,c)$ for any $c \in P_{ob_\kappa}$, which implies that $c \in P_{qr_\kappa}$. Following the second part of the proof of Theorem 2.8, we can show that whenever $c \in P_{qr_\kappa}$, $c \in P_{ob_\kappa}$. Thus, whenever

$$\mu_K(b,o) = \mu_K(r,o), \quad P_{ob_\kappa} = P_{qr_\kappa}.$$

To prove the converse, suppose $P_{ob_\kappa} = P_{qr_\kappa}$. Note that $b \notin P_{ob_\kappa}$, and since $P_{ob_\kappa} = P_{qr_\kappa}$, $b \notin P_{qr_\kappa}$, which implies that

$$\mu_K(q,b) \leq \mu_K(r,b).$$

Since $q \in P_{ob_\kappa}$, by (2.7) $\mu_K(q,b) = \mu_K(b,o)$. Hence,

$$\mu_K(b,o) \leq \mu_K(r,b),$$

and by (2.5) we get,

$$\mu_K(b,o) \leq \mu_K(r,o). \tag{2.17}$$

Analogously, since $r \notin P_{qr_\kappa}$ and so $r \notin P_{ob_\kappa}$, which implies $\mu_K(r,o) \leq \mu_K(b,r)$ and by (2.5) we have,

$$\mu_K(r,o) \leq \mu_K(b,o). \tag{2.18}$$

From (2.17) and (2.18), we arrive at $\mu_K(b,o) = \mu_K(r,o)$.□

The above two theorems have different implications in the practical computation of relative fuzzy κ-objects in a given scene in a repeatable, consistent manner. Although less specific and, therefore, more restrictive, Theorem 2.8 offers practically a more relevant guidance than Theorem 2.9 for selecting spels in the object and background so that the relative fuzzy κ-object defined is independent of the reference spels. Fig. 2b shows a 2D scene that was created from a binary scene (Fig. 2a) of an object of circular shape by applying a Gaussian smoothing filter, noise, and a fixed slow varying (ramp) background component across the columns. For a spel o specified near the center of the circular region and a spel b specified in the background, Fig. 2c shows (in white) the set of spels in the scene domain for which the conditions expressed in (2.15) and (2.16) are violated. That is, if o is chosen to be inside the object region, and b is chosen deep in the background region, both away from the fuzzy boundary of the object, then (2.15) is satisfied and a constancy of the relative fuzzy κ-object to reference spels can be guaranteed.

The result given below follows immediately from (2.16), (2.7), and (2.8).

Corollary 2.10. *For any scene $\mathcal{C} = (C,f)$ over (Z^n,α), for any affinity κ in $\mathcal{C}$, and for any spels o,b,q and r in C such that $q \in P_{ob_\kappa}$, $P_{ob_\kappa} = P_{qr_\kappa}$, if, and only if,*

$$\mu_K(b,o) = \mu_K(b,q) = \mu_K(r,o) = \mu_K(r,q).$$

Proof. Suppose

$$P_{ob_\kappa} = P_{qr_\kappa}.$$

Then, by (2.16), $\mu_K(b,o) = \mu_K(r,o)$. By (2.6), $r \notin P_{qr_\kappa}$ and so $r \notin P_{ob_\kappa}$, and by (2.7),

$$\mu_K(b,o) = \mu_K(b,q)$$

and $\mu_K(r,o) = \mu_K(r,q)$.

Conversely, when

$$\mu_K(b,o) = \mu_K(r,o) (= \mu_K(b,q) = \mu_K(r,q)),$$

by (2.16), $P_{ob_\kappa} = P_{qr_\kappa}$. □

It follows from Theorems 2.8 and 2.9, by setting $q = o$, that $P_{or_\kappa} = P_{ob_\kappa}$. However, the constancy of the relative κ-object, even in this situation where the reference spel for the object is fixed but changeable only for the background, requires constraints expressed in (2.15) and (2.16).

The following theorem states an important property of relative fuzzy κ-objects, namely that their domain, that is the set P_{ob_κ}, is path connected in the sense that for any two spels $q, c \in P_{ob_\kappa}$, the best path between them is entirely contained by P_{ob_κ}. This very desirable property is not satisfied by the method of [30].

Theorem 2.11. *For any scene $\mathcal{C} = (C,f)$ over (Z^n,α), for any affinity κ in $\mathcal{C}$, and for any spels o,b,q and c in C such that $q, c \in P_{ob_\kappa}$, all spels in the best path from q to c are contained in P_{ob_κ}.*

Proof. Suppose that the best path between q and c contains a spel $r \notin P_{ob_\kappa}$. By (2.2) we have $\mu_K(r,c) \geq \mu_K(q,c)$. This, however, contradicts Proposition 2.6. □

3 Theory of Iterative Relative Fuzzy Connectedness

In this section, we describe an iterative framework for defining relative fuzzy connectedness while satisfying the key theoretical results in Section 2. (This key idea was originally presented in a conference proceedings [29].) Prior to this, an intuitive description of the motivation and the key ideas are given using a two-dimensional example.

3.1 An Outline of the Key Ideas

Consider the situation illustrated in Fig. 3 which demonstrates three objects O_1, O_2 and O_3. It is very likely that, for a spel such as c, $\mu_K(o,c) \approx \mu_K(b,c)$ because of the blurring that takes place in those parts where O_1 and O_2 come close together. In this case, the strongest path from b to c is likely to pass through the "core" of O_1 which is indicated by the dotted curve in the figure. This core, which is roughly P_{ob_κ}, can be detected first and then excluded from consideration in a subsequent iteration for any path from b to c to pass through. Then, we can substantially weaken the strongest path from b to c compared to the strongest path from o to c which is still allowed to pass through the core. This leads us to an iterative strategy to grow from o (and so complementarily from b) to more accurately capture O_1 (and O_2) than if a single-shot relative connectedness strategy is used. The phenomenon illustrated in Fig. 3 is general and may be characterized in the following way. Most objects have a core part, which is relatively easy to segment after specifying the seed spel, and other diffused, subtle and fine parts that spread off from the core, which pose segmentation challenges. Although the latter seem to hang together fairly strongly with the core from a visual perceptual point of view, because of the ubiquitous noise and blurring, it is difficult to devise computational means to capture them as part of the same object by using a single-shot strategy. The iterative strategy captures these loose parts in an incremental and reinforcing manner. This formulation is described below.

For any fuzzy affinity κ and any two spels $c, d \in C$, define

$$\mu_{\kappa_{ob}^0}(c,d) = \mu_\kappa(c,d) \tag{3.1}$$

$$P^0_{ob_\kappa} = \{c \mid c \in C \text{ and } \mu_K(o,c) > \mu_{K^0_{ob}}(b,c)\}. \tag{3.2}$$

Note that $P^0_{ob_\kappa}$ is exactly the same as P_{ob_κ}, defined in (2.6). Assuming that $P^{i-1}_{ob_\kappa}$ and κ^{i-1}_{ob} are defined for any positive integer i, $P^i_{ob_\kappa}$, and κ^i_{ob} are defined as follows: For any $c, d \in C$,

$$\mu_{\kappa^i_{ob}}(c,d) = \begin{cases} 1, & \text{if } c = d, \\ 0, & \text{if } c \text{ or } d \in P^{i-1}_{ob_\kappa}, \\ \mu_\kappa(c,d), & \text{otherwise,} \end{cases} \tag{3.3}$$

$$P^i_{ob_\kappa} = \{c \mid c \in C \text{ and } \mu_K(o,c) > \mu_{K^i_{ob}}(b,c)\}. \tag{3.4}$$

An *iteratively defined fuzzy κ^i-object $\mathcal{O}^i$ of a scene $\mathcal{C} = (C, f)$ containing a spel o relative to a background containing a spel b* is a fuzzy subset of C defined by the membership function

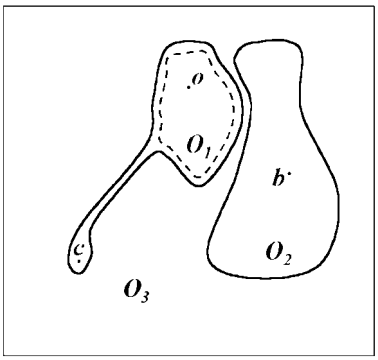

Fig. 3. Illustration of the key ideas behind iterative relative fuzzy connectedness. In the first iteration the core of object O_1, indicated by the dotted curve, is identified within which the strength of connectedness of spels with respect to o is greater than with respect to b. In the second iteration, the affinity of O_2 (and not of O_1) is modified so that any path that goes through the core region in O_1 from b will have zero strength. The new "core" is then determined using relative connectedness and the process continues iteratively until no changes are observed.

$$\mu_{\mathcal{O}^i}(c) = \begin{cases} \eta(f(c)), & \text{if } c \in P^i_{ob_\kappa}, \\ 0, & \text{otherwise.} \end{cases} \tag{3.5}$$

For short, we will refer to $\mathcal{O}^i$ simply as an *iterative relative fuzzy κ^i-object of $\mathcal{C}$*. In the rest of this section, we will explore the properties of $P^i_{ob_\kappa}$ and of $\mathcal{O}^i$ in a manner analogous to those of relative κ-connectedness and relative κ-object established in the previous section.

Proposition 3.1. *For any scene $\mathcal{C} = (C, f)$ over (Z^n, α), for any affinity κ in $\mathcal{C}$, for any spels o and b in C, and for any nonnegative integers $i < j$, $P^i_{ob_\kappa} \subseteq P^j_{ob_\kappa}$.*

Proof. We show by induction that for any positive integer i, $P^{i-1}_{ob_\kappa} \subseteq P^{i+1}_{ob_\kappa}$.

Following (3.1) and (3.3), it is easy to see that, for any spels

$$c, d \in C, \mu_{\kappa^0_{ob}}(c,d) \geq \mu_{\kappa^1_{ob}}(c,d).$$

Therefore, for any path

$$p_{qr} \in P_{\mathcal{C}}, \mu_{\mathcal{N}_{\kappa^0_{ob}}}(p_{qr}) \geq \mu_{\mathcal{N}_{\kappa^1_{ob}}}(p_{qr})$$

so that $\mu_{K^0_{ob}}(c,d) \geq \mu_{K^1_{ob}}(c,d)$. Since c, d are any spels of C, this implies that $\mu_{K^0_{ob}}(b,c) \geq \mu_{K^1_{ob}}(b,c)$. Therefore, from (3.2) and (3.4), $c \in P^0_{ob_\kappa}$ implies that $c \in P^1_{ob_\kappa}$. Hence, $P^0_{ob_\kappa} \subseteq P^1_{ob_\kappa}$.

Now assume that $P^{i-1}_{ob_\kappa} \subseteq P^i_{ob_\kappa}$. From (3.3) and our assumption, for any spels $c, d \in C$, $\mu_{\kappa^i_{ob}}(c,d) \geq \mu_{\kappa^{i+1}_{ob}}(c,d)$. Following an argument analogous to that given in the previous paragraph, it follows that $P^i_{ob_\kappa} \subseteq P^{i+1}_{ob_\kappa}$. □

In the above proposition, we showed essentially that $P^i_{ob_\kappa}$ is noncontracting as iterations continue. In the following proposition, we show that, at any iteration i, $P^i_{ob_\kappa}$ is path connected in the sense that for any spels $c, d \in P^i_{ob_\kappa}$, all spels in at least one of the best paths (with respect to κ) are contained in $P^i_{ob_\kappa}$. That is, if p^i_{cd} is the best path between c and d among those paths all of whose spels are in $P^i_{ob_\kappa}$, then $\mu_{\mathcal{N}_\kappa}(p^i_{cd}) = \mu_K(c,d)$.

Proposition 3.2. *For any scene $\mathcal{C} = (C, f)$ over (Z^n, α), for any affinity κ in $\mathcal{C}$, for any nonnegative integer i and for any spels*

o, b, q, and, c in C such that $q, c \in P^i_{ob_\kappa}$, all spels in at least one best path (with respect to κ) from q to c are contained in $P^i_{ob_\kappa}$.

The proof of this proposition is long and, hence, is not given here. See [37] for a complete proof.

The following proposition shows that $P^i_{ob_\kappa}$ and $P^j_{bo_\kappa}$ maintain their disjoincy at every iteration for any i and j. It will be used later in proving a robustness theorem for iterative fuzzy κ^i-objects in a manner analogous to Theorem 2.8.

Proposition 3.3. *For any scene $\mathcal{C} = (C, f)$ over (Z^n, α), for any affinity κ in $\mathcal{C}$, for any spels o, b in C, and for any nonnegative integers i, j, $P^i_{ob_\kappa} \cap P^j_{bo_\kappa} = \phi$.*

Proof. From (3.1) and (3.2), it readily follows that $P^0_{ob_\kappa} \cap P^0_{bo_\kappa} = \phi$. Therefore, if the proposition is false, there are smallest nonnegative integers i and j for which $P^i_{ob_\kappa}$ intersects $P^j_{bo_\kappa}$. Let c be a spel in $P^i_{ob_\kappa} \cap P^j_{bo_\kappa}$. Since $P^0_{ob_\kappa} \cap P^0_{bo_\kappa} = \phi$, i or j is nonzero. Suppose that $j \neq 0$. Then, $\mu_K(o, c) \geq \mu_K(b, c)$. From Proposition 3.2, there exists a path p_{oc} from o to c such that all spels of p_{oc} are contained in $P^i_{ob_\kappa}$ and $\mu_{\mathcal{N}_\kappa}(p_{oc}) = \mu_K(o, c) \geq \mu_K(b, c)$. Hence, $\mu_{K^j_{bo}}(o, c) \geq \mu_K(b, c)$ unless $P^{j-1}_{bo_\kappa}$ contains a spel in p_{oc}. In that case, $P^{j-1}_{bo_\kappa}$ intersects $P^i_{ob_\kappa}$, contradicting our assumption that j is the smallest integer for which $P^j_{bo_\kappa}$ intersects $P^i_{ob_\kappa}$. When $j = 0, i$ must be nonzero; and the proposition can be proved in the same way as we did for $j \neq 0$. □

The following theorem states an important property of iterative relative fuzzy κ^i-objects and shows their robustness with respect to reference seed spels. It is analogous to Theorem 2.8 on noniterative relative fuzzy κ-objects.

Theorem 3.4. *For any scene $\mathcal{C} = (C, f)$ over (Z^n, α), for any affinity κ in $\mathcal{C}$, for any spels o, b, q, and r in C such that $q \in P_{ob_\kappa}$, and for any nonnegative integer i, $P^i_{ob_\kappa} = P^i_{qr_\kappa}$ if $r \in P_{bo_\kappa}$.*

See [37] for a complete proof.

4 Algorithms

In this section, we present two algorithms. The first, called $\kappa RFOE$, is for extracting a fuzzy κ-object $\mathcal{O}$ of a scene $\mathcal{C} = (C, f)$ containing a spel o relative to a background containing a spel b. The second algorithm, named $\kappa IRFOE$, delineates an iteratively defined fuzzy κ^i-object $\mathcal{O}^i$ of $\mathcal{C}$ containing a spel o relative to a background containing a spel b. We subsequently prove the correctness of both algorithms in terms of their termination and producing the expected output.

Algorithm $\kappa RFOE$

Input: $\mathcal{C} = (C, f)$, κ, spels o and b, and η as defined in Section 2.

Output: Fuzzy κ-object $\mathcal{O}$ containing o relative to a background containing b.

Auxiliary Data Structures: The κ-connectivity scene $\mathcal{C}_{K_o} = (C, f_{K_o})$ of o in $\mathcal{C}$; the κ-connectivity scene $\mathcal{C}_{K_b} = (C, f_{K_b})$ of b in $\mathcal{C}$; a queue Q containing spels to be processed.

begin

0. *for* $x \in \{o, b\}$ *do*
1. set $f_{K_x}(c) = 0$ for all $c \in C$ except for x set $f_{K_x}(c) = 1$;
2. push all spels $c \in C$ such that $\mu_\kappa(x, c) > 0$ to Q;
3. *while* Q is not empty *do*
4. remove a spel c from Q;
5. find $f_{max} = \max_{d \in C}\{\min(f_{K_x}(d), \mu_\kappa(c, d))\}$;
6. *if* $f_{max} > f_{K_x}(c)$ *then*
7. set $f_{K_x}(c) = f_{max}$;
8. push all spels e such that $\mu_\kappa(c, e) > f_{K_x}(e)$ to Q;

endif;

endwhile;

endfor;

9. *for* all $c \in C$ *do*
10. *if* $f_{K_o}(c) > f_{K_b}(c)$ *then* set $\mu_{\mathcal{O}}(c) = \eta(f(c))$;
11. *else* set $\mu_{\mathcal{O}}(c) = 0$;

endfor;

12. output $\mathcal{O}$;

end

In the above algorithm, Steps 0-8 are for computing the connectivity scenes $\mathcal{C}_{K_o}$ and $\mathcal{C}_{K_b}$. In Steps 6-8, whenever a strictly better path up to a spel c is found, the strength of connectedness at c is updated and c is pushed into the queue to pass this information to its neighbor. These are essentially the same as the steps in the algorithm κFOE presented in [3]. Therefore, the fact that, at the end of Step 8, $\kappa RFOE$ indeed produces the two connectivity scenes $\mathcal{C}_{K_o}$ and $\mathcal{C}_{K_b}$ correctly follows from Proposition 3.1 in [3]. Since Steps 9-12 compute the relative fuzzy κ-object from these scenes as per our definition ((2.6), (2.4)), $\kappa RFOE$ indeed behaves correctly producing the correct output.

Proposition 4.1. *For any scene $\mathcal{C} = (C, f)$ over (Z^n, α), for any fuzzy affinity relation κ in $\mathcal{C}$, and for any spels o and b in C, algorithm $\kappa RFOE$ terminates and at that time it outputs the fuzzy κ-object $\mathcal{O}$ containing o relative to the background containing b.*

Algorithm $\kappa IRFOE$

Input: $\mathcal{C} = (C, f)$, κ, spels o and b, and η as defined in Section 2.

Output: Iteratively defined fuzzy κ-object $\mathcal{O}^i$ containing o relative to a background containing b.

Auxiliary Data Structures: The κ-connectivity scene $\mathcal{C}_{K_o} = (C, f_{K_o})$ of o in $\mathcal{C}$; the κ^i_{ob}-connectivity scene $\mathcal{C}_{K^i_{ob}} = (C, f_{K^i_{ob}})$ of b in $\mathcal{C}$.

begin

0. compute $\mathcal{C}_{K_o}$ (using $\kappa RFOE$);
1. set $i = 0$ and $\kappa^i_{ob} = \kappa$;
2. set $flag$ = true, and $count$ = 0;
3. *while* $flag$ is true *do*
4. set $flag$ = false, old_count = $count$, and $count$ = 0;
5. compute $\mathcal{C}_{K^i_{ob}}$ (using κ^i_{ob} as affinity);

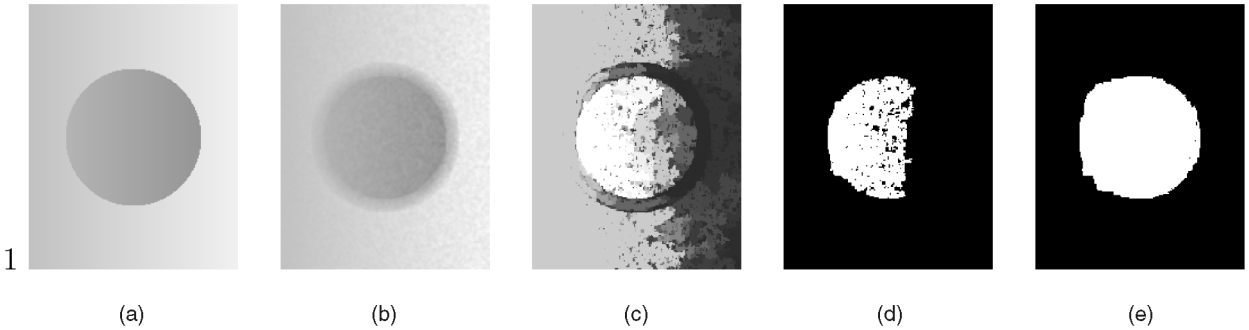

Fig. 4. (a) A 2D scene of a disk whose contrast with the background increases from left to right. (b) The scene of (a) together with noise and blurring. (c) The connectivity scene of the scene in (b) for a spel o selected near the center of the disk. (d) The binary scene resulting from thresholding the scene in (c) at the best possible threshold. (e) The binary scene (the white region represents $P^i_{ob_\kappa}$) resulting from iterative relative fuzzy connectedness, where b was specified on the left side of the disk in the background.

```
6.        set κ^i_ob = κ;
7.        for all c ∈ C do
8.            if f_Ko(c) > f_K^i_ob(c) then
9.                set μ_O^i(c) = η(f(c));
10.               increment count by 1;
11.               for all d ∈ C do
12.                   set μ_κ^i_ob(c, d) = 0;
                  endfor;
13.           else set μ_O^i(c) = 0;
              endif;
          endfor;
14.       if count ≠ old_count then set flag = true;
15.       increment i by 1;
      endwhile;
16.   output O^i;
end
```

Proposition 4.2. *For any scene $\mathcal{C} = (C, f)$ over (Z^n, α), for any fuzzy affinity relation κ in $\mathcal{C}$, and for any spels $o, b \in C$, algorithm $\kappa IRFOE$ terminates in a finite number of steps.*

See [37] for a complete proof.

Proposition 4.3. *For any scene $\mathcal{C} = (C, f)$ over (Z^n, α), for any fuzzy affinity relation κ in $\mathcal{C}$, and for any spels $o, b \in C$, after each iteration, algorithm $\kappa IRFOE$ outputs the iterative fuzzy κ-object $\mathcal{O}^i$ as defined in (3.5).*

See [37] for a complete proof.

5 Experimental Results

In this section, we present several examples to demonstrate the behavior of algorithms $\kappa RFOE$ and $\kappa IRFOE$. We also present a quantitative comparative evaluation of algorithm $\kappa IRFOE$ and the original absolute fuzzy connectedness algorithm κFOE described in [3] based on 160 mathematical phantoms.

The first example, shown in Fig. 4, is a 2D mathematical phantom and is mainly for illustrating the concepts. It was created by blurring a circular disk (using a Gaussian kernel) that was originally generated by adding a contrast that increases from left to right as a ramp function and then by adding noise which also increases from left to right as a ramp function. A background component of variation, also a ramp, was also added. The circular disk and the 2D scene depicting the resulting phantom are shown in Figs. 4a and 4b. Fig. 4c shows the connectivity scene (a seed for the object was specified near the center of the disk) and Fig. 4d shows a binary segmentation achieved via absolute connectedness using the best possible threshold. (This was chosen among all thresholds that yielded a segmentation with the best possible overlap with the original disk.) In this case, it is impossible to set a proper threshold on the strength of connectedness so as to capture the different parts of the object region because of varying noise and contrast within the object region. However, iterative relative fuzzy connectedness achieves a decent segmentation (Fig. 4e) without the need for a threshold. For iterative relative fuzzy connectedness, a spel on the left side of the disk was selected for background. The area of mismatch with the original disk area expressed as a percent of the original disk area for the images in Figs. 4d and 4e are 48.0 percent and 16.5 percent, respectively. Iterative relative fuzzy connectedness automatically determines along best paths such as p_{oc} and p_{bc}, where o and b are reference spels within the object and the background regions, respectively, the spel c at which the strength of p_{oc} just exceeds that of p_{bc}. This strength is likely to be not a fixed threshold but a variable entity in the fuzzy boundary between the object and the background. We may think of the iterative relative fuzzy connectedness method as adaptively changing the threshold of connectedness around the fuzzy boundary. This is the essence and the strength of iterative relative over absolute fuzzy connectedness.

In the following, three experiments taken from real life applications, multiple seeds were utilized to specify objects and different co-objects in the background. A theory for the case of multiple objects is presented in [27]. Our first example, illustrated in Figs. 5 and 6, is taken from MR angiography. The problem here is the separation of arteries and veins in contrast-enhanced MRA images. MR imaging approaches exist [38] which attempt to elicit different types of signals from arteries and veins through carefully designed imaging protocols and thereby to distinguish arteries from veins. Ours is a postprocessing approach based on MR images that are acquired using long-resident blood-pool contrast agents [39] which do not give different signals from the arteries and veins but which provide a better overall definition of the vessels themselves.

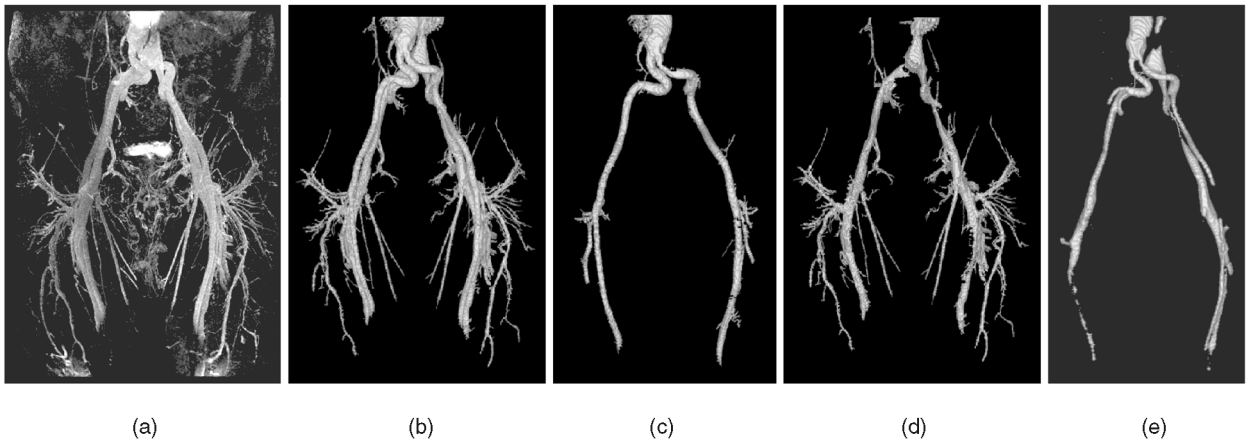

Fig. 5. (a) A MIP rendition of an MRA scene from a patient. (b) The whole vascular tree segmented via fuzzy connectedness from the scene depicted in (a). (c) The arterial tree separated from the whole vascular tree of (b) via iterative relative fuzzy connectedness. (d) Analogous to (c) but for the veinous tree. (e) The veinous tree obtained by thresholding the connectivity scene for the whole vascular tree. Note that the images in (b), (c), (d), and (e) are renditions of the 3D fuzzy objects obtained by respective segmentation strategies.

Figs. 5a and 6a show a maximum intensity projection (MIP) rendering from each of two MRA scenes (of size $512\times512\times60$ and $432\times512\times60$, both with $0.94\times0.94\times1.8\ \mathrm{mm}^3$ voxel size) acquired from two patients in the region from their belly to knee. (MIP rendering does not involve any segmentation. In this method, the voxel with the highest intensity along each projection line is assigned to a pixel in the rendition.) Figs. 5b and 6b show a shell rendition [40] (a method of rendering fuzzy objects) of the whole fuzzy vascular structure that was segmented using absolute fuzzy connectedness from the two data sets. Figs. 5c and 6c show renditions of the fuzzy arterial tree, and Figs. 5d and 6d show renditions of the fuzzy veins for the two data sets separated via iterative relative fuzzy connectedness. Note that, in this experiment, iterative relative fuzzy connectedness was applied between arteries and veins so that when the arterial tree was segmented the veinous tree served as the background and vice versa. In these experiments seeds were selected in a semiautomatic manner [19]. The user selected a few seed spels in the major segments of the artery and vein. The best (strongest) path passing through these spels was then computed, and all spels in that path were considered to be the seed spels. In all cases, the iterations stopped after four loops. For comparison, we show in Figs. 5e and 6e the renditions of the vein detected from the two data sets using absolute fuzzy connectedness. Here, we selected the best threshold as visually determined from thresholding the respective connectivity scenes. As seen in comparison with Figs. 5d and 6d, the separation of the veins is very unsatisfactory in Fig. 5e and 6e. These relative connectedness algorithms are part of a package that we have developed, called 3DVIEWNIX-AVS, for routine artery/vein separation in clinical MRA. (3DVIEWNIX [41] is a software system developed, maintained and distributed by us for the visualization, processing, and analysis of multidimensional scenes.) Further, over 200 MRA data sets coming from six different hospitals have been processed in this fashion and shown to work correctly. Two of these data sets were manually segmented by experts (interventional radiologists). A comparison of the results revealed that our algorithm's results agreed with the experts' segmentation up to the second order branches. Manual segmentation beyond the second order branches was impossible. However the algorithms separated and delineated the higher order branches correctly as determined by the experts from the volume renditions of the algorithmic results.

Two more examples are illustrated in Figs. 7 and 8. Fig. 8a displays an axial color slice from the visible human data of a female cadaver. These data were generated by the National Library of Medicine by axially slicing the frozen cadaver of a female at every plane $0.3\ \mathrm{mm}$ apart and then acquiring a color digital photographic image of the cross section. The in-plane resolution of the image is $0.3\times0.3\ \mathrm{mm}^2$. The slice shown in the figure is taken from the mid-brain region. We applied iterative relative fuzzy connectedness to segment the white matter region from the rest of the tissues in the particular slice. Fig. 7b displays the result. In this experiment, fuzzy affinity was computed using a fully vectorial analysis of the scene with three orthogonal color components, namely, red, green, and blue for every pixel. A detailed description of affinity computation for vectorial images is presented in [42]. As illustrated in Fig. 7b, the method successfully segmented the white matter region preserving very fine details. In this experiment, seeds were manually specified within the white matter region for object and within gray matter region and cerebro spinal fluid for background. These seeds are shown on the image (blue dots for objects and white dots for the background). Another example of color image segmentation is presented in Fig. 8b,[1] Fig. 8 displays a color digital photographic image of a sculpture acquired in the natural day light scene. Fig. 8b shows the result of segmentation of the sculpture from the rest of the scene. Here too, fuzzy affinity was computed in a fully vectorial fashion considering the three color components. As in Fig. 8b, the result of segmentation of the sculpture is visually acceptable. In this experiment, one seed was used for the sculpture (object) and one seed for each region in the background. These seeds are shown in the figure. Note that, in both cases, the set of all objects

1. The image was copied from the following Website: http://www.bluffton.edu/HomePages/FacStaff/sullivanm/viennamuseumgiacometti.jpg. The authors are grateful to the owner of this Website.

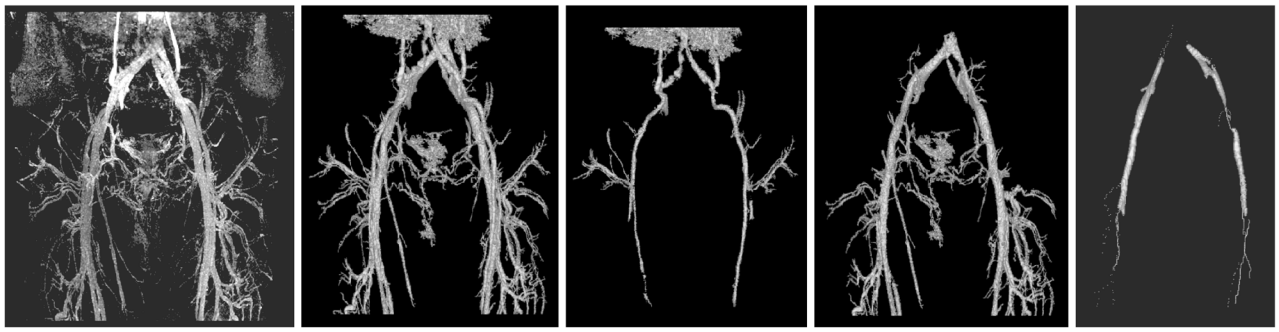

(a) (b) (c) (d) (e)

Fig. 6. Same as Fig. 5 but for a different patient.

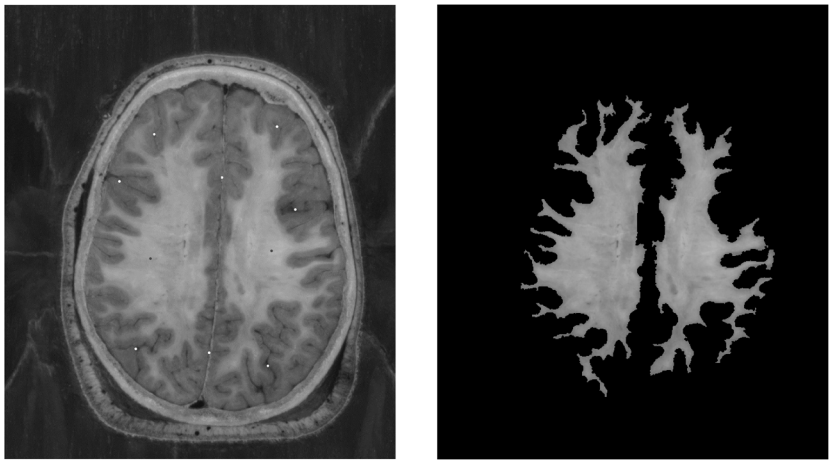

(a) (b)

Fig. 7. (a) An axial slice taken from the midbrain region from the color cryosection female visible human data. (b) White matter regions segmented by using iterative relative fuzzy connectedness on the color vectorial scene. Seeds for object are shown by dots while those for background are shown by dots.

other than the object of interest was considered to represent the co-object. The final example, illustrated in Figs. 9, 10, and Tables 1, 2, and 3 consists of a set of 160 mathematical phantom images. Our aim here is to do a quantitative comparison between absolute and relative fuzzy connectedness. The phantom scenes are generated from 10 different patient 3D MR studies of the brain. One transaxial slice, approximately at the same location in the brain is selected from each of these 10 3D scenes. Each of these 10 2D scenes is segmented carefully to separate the white matter region using a user steered segmentation method [11]. In this boundary-based approach, optimal boundary segments are determined by an algorithm between user selected points on the boundary of the object. From this information, from each of the original 10 2D scenes, a new 2D scene is generated by assigning to pixels in the white matter region a constant intensity equal to the average of the intensities within the same segmented white matter region in the corresponding original MR 2D scene. A "gray matter background" is provided in the simulated 2D scene by separately segmenting the brain parenchymal region and by assigning to this region a constant intensity equal to the average of the intensities within the same background region in the corresponding original MR 2D scene. From this set of 10 simulated 2D scenes, we created a total of 160 2D scenes by blurring (using a 2D Gaussian kernel) each 2D scene in this set to four different degrees of blurring and by adding a 0-mean Gaussian correlated noise component at four different levels. Each of these 160 2D scenes is further modified by adding a fixed slow varying (ramp) background component which changed from 0 at the first column to 100 at the last column in the 2D scene. This new set of 2D scenes, denoted

$$E = \{\mathcal{C}_i \mid \mathcal{C}_i = (C, f_i), 1 \leq i \leq 160\},$$

is utilized in our experiments. Three samples from this set are displayed in Figs. 9a, 9b, and 9c. Object-background difference for the examples of Fig. 9 are in the range [120, 150]. Standard deviations of the correlated zero-mean Gaussian noise used in the examples are low = 10, medium = 15, high = 25. Standard deviations for the Gaussian blurring kernels (each of size $6\times$ standard deviation + 1) used for the three examples are low = 1.5, medium = 2.0, and high = 3.0.

Let $E_b = \{\mathcal{C}_{bi} \mid \mathcal{C}_{bi} = (C, f_{bi}), 1 \leq i \leq 160\}$ be the set of binary scenes such that, for $1 \leq i \leq 160$, $\mathcal{C}_{bi}$ represents the original segmentation of the white matter region

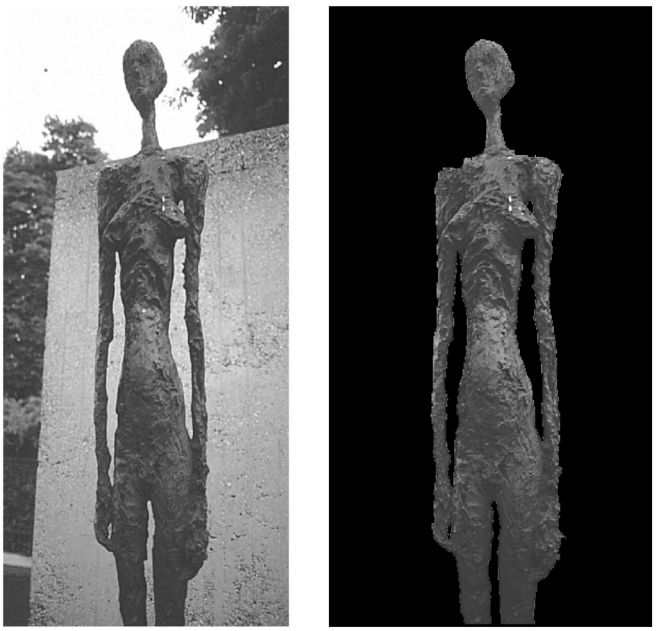

(a) (b)

Fig. 8. Please the digital library for a color representation. (a) In the color figure shows a digital color photographic image of a sculpture in a natural daylight scene. (b) In the color figure show the sculpture segmented from the rest of the natural scene by using iterative relative fuzzy connectedness on the color vectorial scene. Seeds for sculpture are shown by yellow dots while those for background are shown by red dots.

corresponding to the simulated scene $\mathcal{C}_i$ in E. Scenes in E_b will be used as true segmentations. We denote by $E_a = \{\mathcal{C}_{ai} \mid \mathcal{C}_{ai} = (C, f_{ai}), 1 \leq i \leq 160\}$ the set of binary scenes produced by the absolute connectedness method and by $E_r = \{\mathcal{C}_{ri} \mid \mathcal{C}_{ri} = (C, f_{ri}), 1 \leq i \leq 160\}$ the set of binary scenes produced by the relative connectedness method from the set E of input scenes.

In the following, for any scene $\mathcal{C} = (C, f)$, we denote by $\mathcal{C}^t = (C, f^t)$ the binary scene resulting from thresholding $\mathcal{C}$ at t. That is, for any $c \in C$ $f^t(c) = 1$, if $f(c) \geq t$, 0 otherwise. We define figures of merit FOM_{ai} and FOM_{ri} for the accuracy of segmentation for the two methods, which constitute the degree of overlap between the segmentation results and the true segmentation, as follows; For $1 \leq i \leq 160$,

$$FOM_{ai} = \max_t \left[\left(1 - \frac{|\mathcal{C}_{ai}^t \ EOR \ \mathcal{C}_{bi}|}{|C|} \right) \times 100 \right], \quad (5.1)$$

$$FOM_{ri} = \left[\left(1 - \frac{|\mathcal{C}_{ri} \ EOR \ \mathcal{C}_{bi}|}{|C|} \right) \times 100 \right], \quad (5.2)$$

where $|C|$ is the cardinality of C, EOR represents the Exclusive OR operation between the two binary scenes and $|\mathcal{C}_{xi}^t \ EOR \ \mathcal{C}_{bi}|$ denotes the number of 1-valued pixels in $\mathcal{C}_{xi}^t \ EOR \ \mathcal{C}_{bi}$ for $x \in \{a, r\}$. FOM_{ai} represents the best possible degree of match between the original (true) white matter object region captured in $\mathcal{C}_{bi}$ and the white matter object region in $\mathcal{C}_{ai}$ over all possible thresholds t on $\mathcal{C}_{ai}$. In this fashion, our comparison becomes independent of how the connectivity scenes are thresholded for the absolute connectedness method. However, it must be pointed out that in practical segmentation tasks, this optimum cannot be achieved since true segmentation is not known.

Fig. 10 shows one of the scenes from the set E_b in 10a, the corresponding scene from the set E in 10b, the resulting connectivity scene from the set E_a in 10c, the optimally thresholded version of this connectivity scene in 10d, and the binary segmentation resulting from relative connectedness in 10e. Tables 1 and 2 list in each cell the mean and the standard deviation of FOM_{ai} and FOM_{ri}, respectively, for each degree of blurring and noise for the 10 scenes. The degree of blurring and noise increases along rows and columns, respectively. We may make the following observations from the tables. FOM_{ai} is generally greater than FOM_{ri}, although the latter is very close to the former except for the very high level of noise and blurring (row 4, column 4). In other words, relative connectedness not only obviates the need for a threshold but also achieves a level of performance that is close to the theoretical optimum that can be achieved via absolute connectedness. Here closeness is in the same sense as that expressed by the FOMs; that is, in terms of the degree of overlap in segmentations. We wish to emphasize again that, in practice, since true segmentation is not known, the ideal threshold that gave the optimum performance depicted in Table 1 cannot be determined. This is well illustrated by the qualitative comparison displayed in Figs. 5d, 5e, 6d, and 6e. We may also note that the performance of the relative connectedness method seems to be less affected by noise than by blurring, as seen from the entries in the first column of Tables 1 and 2.

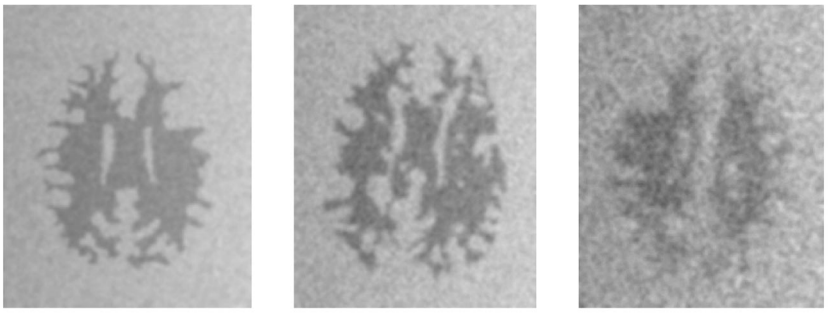

(a) (b) (c)

Fig. 9. Three representative samples from the 160 2D scenes created by adding blurring, noise, and background variation to the binary scenes resulting from user steered segmentation of 10 MRI slices of 10 different patient brain data sets. The levels of blurring and noise in these scenes are (a) low, (b) medium, (c) high.

Fig. 10. (a) One of the original binary scenes from the set E_b. A seed (cross) was manually selected in the object region and three seeds (dots) in the background. (b) The scene resulting after adding noise, blurring and background variation to the scene in (a). (c) The connectivity scene for the spel specified in the object. (d) The binary scene resulting from thresholding the scene in (c) at the best possible threshold. (e) The binary scene (i.e., the set P_{ob_k}) resulting from relative fuzzy connectedness segmentation.

6 Concluding Remarks

We have introduced two new concepts related to fuzzy connectedness in this paper—relative and iterative relative fuzzy connectedness. In relative fuzzy connectedness, the central idea is to define objects based on the relative strength of connectedness of spels with respect to different reference spels specified in the different objects. Thus, objects compete among themselves to win membership of every spel in the scene. A spel c is assigned to that object with respect to whose reference spel c is most strongly connected. We presented a theory of this framework and demonstrated that, as long as the reference spels are selected away from the fuzzy boundary between object regions, the resulting segmentation is independent of the actual reference spels selected. This robustness property is crucial in practical image segmentation. Although the theory was presented considering two objects for simplicity, it can be generalized to any number of objects as demonstrated in [27]. We also presented an algorithm for segmenting objects based on relative fuzzy connectedness which also readily generalizes to multiple objects.

The idea behind iterative relative connectedness actually emerged from our close observation of some of the difficulties encountered in practical segmentation utilizing absolute fuzzy connectedness. The key idea here is to define the "core" parts of the individual objects using relative connectedness with a rather conservative affinity and subsequently to disallow connectivity paths of other objects to pass through the core of each object. In this fashion, the affinity as a relation changes in successive iterations although the functional form remains the same. We have proved the robustness of segmentation to reference spels for this approach also, demonstrated that the iterative process converges, and presented an algorithm for achieving this segmentation. The theory and algorithms are presented for the two-object case and can be generalized with some effort to the case of multiple objects. See [27] for an example.

The power of absolute fuzzy connectedness in image segmentation has been amply demonstrated in the literature in several applications utilizing 1,000s of scenes. In this paper, we have 1) further extended the fuzzy connectedness theoretical framework, 2) obviated the need for a threshold that is required by absolute fuzzy connectedness, and 3) demonstrated the improved effectiveness of relative and iterative relative connectedness in segmentation. One drawback, however, of the relative connectedness framework as presented here is that the affinity relation used for the

TABLE 1
The Mean (First Entry) and Standard Deviation (Second Entry) of FOM_{ai} Values Are Shown in Each Cell for Different Blurring and Noise Conditions

	$Blur\ 1$	$Blur\ 2$	$Blur\ 3$	$Blur\ 4$
$Noise\ 1$	99.007	98.261	97.562	95.803
	0.032	0.097	0.201	0.449
$Noise\ 2$	98.942	98.086	97.321	95.684
	0.026	0.094	0.200	0.446
$Noise\ 3$	98.597	97.662	96.859	95.197
	0.070	0.117	0.235	0.549
$Noise\ 4$	97.429	96.346	95.472	93.673
	0.239	0.348	0.468	0.815

Blurring increases along rows from left to right, while noise increases along columns from top to bottom.

TABLE 2
The Mean (First entry) and Standard Deviation (Second Entry) of FOM_{ri} Values Are Shown in Each cell for Different Blurring and Noise Conditions

	$Blur\ 1$	$Blur\ 2$	$Blur\ 3$	$Blur\ 4$
$Noise\ 1$	98.817	97.582	96.615	94.818
	0.051	0.195	0.394	0.662
$Noise\ 2$	98.724	97.376	96.316	93.536
	0.076	0.285	0.439	6.982
$Noise\ 3$	98.515	96.971	95.632	92.321
	0.082	0.446	0.535	9.023
$Noise\ 4$	97.584	95.338	92.978	86.482
	0.471	1.648	5.174	29.593

Blurring increases along rows from left to right, while noise increases along columns from top to bottom.

TABLE 3
The Mean (First Entry) and Standard Deviation (Second Entry) of FOM_{ri} Values Are Shown in Each Cell for Different Blurring and Noise Conditions

	$Blur\ 1$	$Blur\ 2$	$Blur\ 3$	$Blur\ 4$
$Noise\ 1$	99.376	98.301	97.528	95.872
	0.022	0.089	0.174	0.479
$Noise\ 2$	99.226	98.171	97.341	95.668
	0.026	0.105	0.203	0.512
$Noise\ 3$	98.950	97.857	96.974	95.188
	0.039	0.124	0.214	0.530
$Noise\ 4$	98.194	96.849	95.796	94.024
	0.105	0.218	0.361	0.635

Blurring increases along rows from left to right, while noise increases along columns from top to bottom.

different objects must be the same. This restriction somewhat compromises the effectiveness of the segmentation that can be achieved. As illustrated in Table 3, when different affinities—those that are tailored to the individual objects—are utilized, the resulting segmentations are greatly improved, even over the theoretically optimum segmentation that can be achieved using absolute fuzzy connectedness. Table 3 is analogous to Table 2 except that the FOMs are computed now using segmentations resulting from separate affinities devised for the object region and the background. Note the FOMs in Table 3 are generally superior to those in Table 1. There are several ways of achieving a single affinity relation from affinities that are tailored to the individual object regions in an image. See [27] for an example. We are currently investigating the theoretical, algorithmic and application aspects of this approach. Once this is accomplished, we believe that a truly powerful multiobject segmentation paradigm results.

ACKNOWLEDGMENTS

The authors are grateful to the EPIX Medicals Inc. for the 3D MRA data sets and to Dr. Tianhu Lei for the experimental results involving these data. The work of the authors is supported by grants LM 0-3502-M0D3, NS 37172, and AR 46902 from the National Instituites of Health (NIH).

REFERENCES

[1] Z.H. Cho, J.P. Jones, and M. Sing, *Foundation of Medical Imaging.* New York: John Wiley & Sons, 1993.
[2] N.R. Pal and S.K. Pal, "A Review of Image Segmentation Techniques," *Pattern Recignition,* vol. 26, pp. 1277-1294, 1993.
[3] J.K. Udupa and S. Samarasekera, "Fuzzy Connectedness and Object Definition: Theory, Algorithms, and Applications in Image Segmentation," *Graphical Models and Image Processing,* vol. 58, pp. 246-261, 1996.
[4] S. Raya, "Low-Level Segmentation of 3-D Magnetic Resonance Brain Images—A Rule-Based System," *IEEE Trans. Medical Imaging,* vol. 9, pp. 327-337, 1990.
[5] L. Gong and C. Kulikowski, "Composition of Image Analysis Processes through Object-Centered Hierarchical Planning," *IEEE Trans. Pattern Analysis and Machine Intelligence,* vol. 17, pp. 997-1009, 1995.
[6] M. Kamber, R. Singhal, D. Collins, G. Francis, and A. Evans, "Model-Based 3D Segmentation of Multiple Sclerosis Lesions in Magnetic Resonance Brain Images," *IEEE Trans. Medical Imaging,* vol. 4, pp. 442-453, 1995.
[7] J. Gee, M. Reivich, and R. Bajcsy, "Elastically Deforming 3D Atlas to Match Anatomical Brain Images," *J. Computer Assisted Tomography,* vol. 17, pp. 225-236, 1993.
[8] G. Christensen, R. Rabbitt, and M. Miller, "3-D Brain Mapping Using a Deformable Neuroanatomy," *Physical Medical Biology,* vol. 39, pp. 609-618, 1994.
[9] U Montanari, "On the Optimal Detection of Curves in Noisy Pictures," *Comm. ACM,* vol. 14, pp. 335-345, 1971.
[10] J. Cappelletti and A Rosenfeld, "Three-Dimensional Boundary Following," *Computer Vision Graphics and Image Processing,* vol. 48, pp. 80-92, 1989.
[11] A.X. Falcão, J.K. Udupa, S. Samarasekera, and S. Sharma, "User-Steered Image Segmentation Paradigms: Live Wire and Live Lane," *Graphical Models Image Processing,* vol. 60, pp. 233-260, 1998.
[12] N. Otsu, "A Threshold Selection Method from Gray-Level Histogram," *IEEE Trans. Systems, Man, and Cybernetics,* vol. 9, pp. 62-66, 1979.
[13] T. Hong and A. Rosenfeld, "Compact Region Extraction Using Weighted Pixel Linking in a Pyramid," *IEEE Trans. Pattern Analysis and Machine Intelligence,* vol. 6, pp. 222-229, 1984.
[14] H. Soltanian-Zadeh, J. Windham, and D. Peck, "A Comparative Analysis of Several Transformations for Enhancement and Segmentation of Magnetic Images," *IEEE Trans. Medical Imaging,* vol. 11, pp. 302-318, 1992.
[15] J.K. Udupa, L. Wei, S. Samarasekera, Y. Miki, M.A. van Buchem, and R.I. Grossman, "Multiple Sclerosis Lesion Quantification Using Fuzzy Connectedness Principles," *IEEE Trans. Medical Imaging,* vol. 16, pp. 598-609, 1997.
[16] S. Samarasekera, J.K. Udupa, Y. Miki, and R.I. Grossman, "A New Computer-Assisted Method for Enhancing Lesion Quantification in Multiple Sclerosis," *J. Computer Assisted Tomography,* vol. 21, pp. 145-151, 1997.
[17] Y. Miki, R.I. Grossman, J.K. Udupa, M.A. van Buchem, L. Wei, M.D. Philips, U. Patel, J.C. McGown, and D.L. Kolson, "Differences Between Relapsing Remitting and Chronic Progressive Multiple Sclerosis as Determined with Quantitative MR Imaging," *Radiology,* vol. 210, pp. 769-774, 1999.
[18] B.L. Rice and J.K. Udupa, "Clutter-Free Volume Rendering for Magnetic Resonance Angiography Using Fuzzy Connectedness," *Int'l J. Imaging Systems and Technology,* vol. 11, pp. 62-70, 2000.
[19] T. Lei, J.K. Udupa, P.K. Saha, and D. Odhner, "Artery-Vein Separation via MRA—An Image Processing Approach," *IEEE Trans. Medical Imaging,* vol. 20, pp. 689-703, 2001.
[20] P.K. Saha, J.K. Udupa, E.F. Conant, D.P. Chakraborty, and D. Sullivan, "Breast Tissue Density Quantification via Digitized Mammograms" *IEEE Trans. Medical Imaging,* vol. 20, pp. 792-803, 2001.
[21] J.K. Udupa, J. Tian, D. Hemmy, and P. Tessier, "A Pentium PC-Based Craniofacial 3D Imaging and Analysis System," *J. Craniofacial Surgery,* vol. 8, pp. 333-339, 1997.
[22] R. Cannon, J. Dave, and J. Bezdek, "Efficient Implementation of the Fuzzy *c*-means Clustering Algorithms," *IEEE Trans. Pattern Analysis and Machine Intelligence,* vol. 8, pp. 248-255, 1986.
[23] L. Hall, A. Bensaid, L. Clarke, R. Velthuizen, M. Silbiger, and J. Bezdek, "A Comparison of Neural Networks and Fuzzy Clustering Techniques in Segmenting Magnetic Resonance Images of the Brain," *IEEE Trans. Neural Networks,* vol. 3, pp. 672-683, 1992.
[24] A. Rosenfeld, "Fuzzy Digital Topology," *Information Control,* vol. 40, pp. 76-87, 1979.
[25] I. Bloch, "Fuzzy Connectivity and Math. Morphology," *Pattern Recognition Letters,* vol. 14, pp. 483-488, 1993.
[26] S. Dellepiane and F. Fontana, "Extraction of Intensity Connectedness for Image Processing," *Pattern Recognition Letters,* vol. 16, pp. 313-324, 1995.
[27] P.K. Saha and J.K. Udupa, "Relative Fuzzy Connectedness among Multiple Objects: Theory, Algorithms, and Applications in Image Segmentation," *Computer Vision and Image Understanding,* vol. 82, pp. 42-56, 2001.
[28] J.K. Udupa, P.K. Saha, and R.A. Lotufo, "Fuzzy Connected Object Definition in Images with Respect to Co-Objects," *Proc. Int'l Soc. for Optical Eng. (SPIE) Conf. Medical Imaging,* vol. 3661, pp. 236-245, 1999.

[29] P.K. Saha and J.K. Udupa, "Iterative Relative Fuzzy Connectedness and Object Definition: Theory, Algorithms, and Applications in Image Segmentation," *Proc. IEEE Workshop Math. Methods in Biomedical Image Analysis,* pp. 28-35, 2000.
[30] G.T. Herman and B.M. De Carvalho, "Multiseeded Segmentation Using Fuzzy Connectedness," *IEEE Trans. Pattern Analysis and Machine Intelligence,* vol. 23, pp. 460-474, 2001.
[31] A. Kaufmann, *Introduction to the Theory of Fuzzy Subsets,* vol. 1, New York: Academic Press, 1975.
[32] P.K. Saha, J. K. Udupa, and D. Odhner, "Scale-Based Fuzzy Connected Image Segmentation: Theory, Algorithms, and Validation," *Computer Vision and Image Understanding,* vol. 77, pp. 145-174, 2000.
[33] S.M. Pizer, D. Eberly, D.S. Fritsch, and B.S. Morse, "Zoom-Invariant Vision of Figural Shape: the Mathematics of Cores," *Computer Vision and Image Understanding,* vol. 69, no. 1, pp. 55-71, 1998.
[34] J.H. Elder and S.W. Zucker, "Local Scale Control for Edge Detection and Blur Estimation," *IEEE Trans. Pattern Analysis and Machine Analysis,* vol. 20, pp. 699-716, 1998.
[35] P. Liang and Y.F. Wang, "Local Scale Controlled Anisotropic Diffusion with Local Noise Estimate for Image Smoothing and Edge Detection," *Proc. Int'l Conf. Computer Vision,* pp. 193-200, 1998.
[36] M. Tabb and N. Ahuja, "Multiscale Image Segmentation by Integrated Edge and Region Detection," *IEEE Trans. Image Processing,* vol. 6, no. 5, pp. 642-655, 1997.
[37] P.K. Saha and J.K. Udupa, "Iterative Relative Fuzzy Connectedness and Object Definition: Theory, Algorithms, and Applications in Image Segmentation," TR: MIPG-269, Medical Image Processing Group, Dept. Radiology, Univ. of Pennsylvania, Philadelphia, 2000.
[38] D.A. Bluemke, R.D. Darrow, R. Gupta, S.K. Tadikonda, and C.L. Dormoulin, "3D Contrast Enhanced Phase Contrast Angiography: Utility for Artery/Vein Separation," *ISMRM Proc.,* vol. 2, p. 1237, 1999.
[39] T. Lei, J.K. Udupa, P.K. Saha, D. Odhner, R. Baum, S.T. Tadikonda, and E.K. Yucel, "3D MRA Visualization and Artery-Vein Separation Using Blood-Pool Contrast Agent MS-325," *Academic Radiology,* vol. 9 (suppl. 1), pp. S127-S133, 2002.
[40] J.K. Udupa and D. Odhner, "Shell Rendering," *IEEE Computer Graphics and Applications,* vol. 13, pp. 58-67, 1993.
[41] J.K Udupa, D. Odhner, S. Samarasekera, R.J. Goncalves, K. Iyer, K. Venugopal, and S. Furuie, "3DVIEWNIX: An Open, Transportable, Multidimensional, Multimodality, Multiparametric Imaging System," *Proc. Int'l Soc. for Optical Eng. (SPIE) Conf.,* vol. 2164, pp. 58-73, 1994.
[42] Y. Zhuge, J.K. Udupa, and P.K. Saha, "Vectorial Scale Based Fuzzy Connectedness for Segmenting Anatomical Structures in Visible Human Color Data Sets," *Proc. Int'l Soc. for Optical Eng. (SPIE), Conf. Medical Imaging,* 2002.

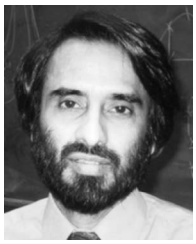

Jayaram K. Udupa received the PhD degree in computer science in 1976 from the Indian Institute of Science, Bangalore, with a medal for best research. During the past 25 years, he has worked in the areas of biomedical image and signal processing, pattern recognition, biomedical computer graphics, 3D imaging, visualization, and their biomedical applications. He has published more than 110 journal papers in these areas, more than 120 full conference papers, edited two books on medical 3D imaging, written more than 20 book chapters and editorials, given more than 120 invited talks (since 1986). He has offered consultancy to several industries, organized conferences, seminars and workshops, and developed the first ever software package for medical three-dimensional imaging and codeveloped and widely distributed large software systems for 3D imaging. He is a fellow of the American Institute of Medical and Biological Engineering. He is at present the Chief of the Medical Imaging Section and Professor of Radiological Sciences in the Department of Radiology at the University of Pennsylvania, Philadelphia. He is a senior member of the IEEE.

Punam K. Saha received the Bachelor's and Master's degrees in computer science and engineering from Jadavpur University, India, in 1987 and 1989, respectively. In 1997, he received the PhD degree from the Indian Statistical Institute, which he joined as a faculty member in 1993. In 1997, he joined the University of Pennsylvania, Department of Radiology, Medical Imaging Section, as a post-doctoral fellow, he is currently an assistant professor. His present research interests include biomedical imaging problems and the application of their solutions, digital topology, and its application to image processing, and estimation of trabecular bone strength from MR images. He has published more than 30 papers in international journals. He received a Young Scientist award from the Indian Science Congress Association in 1996. He is a member of the IEEE and the International Association for Pattern Recognition and a member of the Governing body of the Indian Unit for Pattern Recognition and Artificial Intelligence.

Roberto A. Lotufo received the electronic engineering Diploma from Instituto Tecnologico de Aeronautica, Brazil, in 1978, the MSc degree from State University of Campinas, UNICAMP, Brazil, in 1981, and the PhD degree from the University of Bristol, UK, in 1990, all in electrical engineering. Since 1981, he has been with the Department of Computer Engineering and Industrial Automation, at State University of Campinas (UNICAMP), Brazil. His principal interests are in the areas of image processing applications, multidimensional image processing and analysis, mathematical morphology, and medical imaging.